

# Bacterial Biofilm in Salivary Gland Stones: Cause or Consequence?

Massimo Fusconi, MD<sup>1</sup>, Vincenzo Petrozza, MD<sup>2</sup>,  
Serena Schippa, BD<sup>3</sup>, Marco de Vincentiis, MD<sup>1</sup>,  
Giuseppe Familiari, MD<sup>5</sup>, Fabrizio Pantanella, MD<sup>3</sup>,  
Mirko Cirenza, MD<sup>2</sup>, Valerio Iebba, MD<sup>3</sup>, Ezio Battaglione, MD<sup>5</sup>,  
Antonio Greco, MD<sup>1</sup>, Camilla Gallipoli, MD<sup>4</sup>,  
Flaminia Campo, MD<sup>1</sup>, and Andrea Gallo, MD<sup>4</sup>

No sponsorships or competing interests have been disclosed for this article.

Accepted November 24, 2015.

## Abstract

**Objective.** The pathogenesis of salivary calculi is not yet clear; however, 2 theories have been formulated: (1) “the classic theory,” based on calcium microdeposits in serous and ductal acinous cells, successively discharged into the ducts; (2) “the retrograde theory,” based on a retrograde migration of food, bacteria, and so on from the oral cavity to the salivary duct. The aim of the present study is to highlight the role of bacteria and biofilm in stone formation.

**Study Design.** Case series without comparison.

**Setting.** Laboratory of the Department of Anatomical Pathology.

**Subjects and Methods.** Traditional optic microscopy and scanning electron microscopy were carried out on 15 salivary gland calculi that were collected from 12 patients. A qPCR (quantitative real-time polymerase chain reaction) assay was performed to highlight the presence of bacterial DNA on each stone.

**Results.** Optic microscopy showed formations that—due to their size, shape, and Gram and Giemsa staining—seemed to be Gram-positive bacterial cells. PAS- (periodic acid-Schiff) and alcian-PAS-positive staining matrix was present around them. The ultrastructural observation of the material processed for scanning electron microscopy showed the presence of structures resembling bacterial cells in the middle of the stones, surrounded by soft, amorphous material. Results of qPCR showed the presence of bacterial DNA in the internal part of the tissue sample.

**Conclusions.** The presence of bacteria and/or bacterial products resembling biofilm in salivary gland stones supports the “retrograde theory.” This evidence may support the hypothesis that biofilm could be the causative effect of lithiasic formations.

## Keywords

biofilm, sialolithiasis, optical microscope, SEM, qPCR

The pathogenesis of salivary calculi is still under investigation. Currently, the classic theory, proposed by Harrison, is the most favored one, suggesting that within the serous and ductal acinous cells, calcium microdeposits/microconcretions are produced and discharged into the ducts, especially through gland inactivity forming inorganic calcium nuclei.<sup>1,2</sup>

Marchal et al, as well as other authors, have recently proposed a new theory,<sup>3</sup> “the retrograde theory,” based on migration of food, bacteria, and/or bacterial components and foreign objects from the oral cavity to the salivary duct. Migration is facilitated by functional instabilities of the sphincter.<sup>3-6</sup>

Cofactors associated with salivary gland stone formation are the decrease in salivary flow, dehydration, and salivary pH variations, secondary to pharyngeal infections.<sup>3</sup> Also, in salivary gland stones, an organic matrix was detected.<sup>7,8</sup> Both theories suggest that an organic base is necessary for the formation of calculi: glycoprotein precipitate is produced by cells in the classic theory and a highly saturated mucous plug solution composed of carbohydrates and amino acids in the retrograde theory.

<sup>1</sup>Department of Sensory Organs, ENT Clinic, Sapienza University of Rome, Rome, Italy

<sup>2</sup>Department of Medical and Surgical Sciences and Biotechnologies, Faculty of Pharmacy and Medicine, Sapienza University of Rome, Latina, Italy

<sup>3</sup>Department of Public Health and Infectious Diseases, Microbiology Section, Sapienza University of Rome, Rome, Italy

<sup>4</sup>Department of Medical-Surgical Biotechnologies and Science, ENT, Sapienza University of Rome, Latina, Italy

<sup>5</sup>Department of Anatomical Pathology, Forensic and Locomotor Apparatus Sciences, Sapienza University of Rome, Rome, Italy

## Corresponding Author:

Massimo Fusconi, MD, Department of Sensory Organs, Sapienza University of Rome, Viale del Policlinico, 151-00161 Rome, Italy.  
Email: massimo.fusconi@libero.it

The inorganic component is composed of phosphate calcium under the form of magnesium-hydroxylapatite, ammonium carbonate, and ions.<sup>7</sup> Through the use of a universal bacterial primer, a region of the 16s RNA bacterial gene was detected by polymerase chain reaction (PCR) in salivary gland calculi,<sup>9</sup> and the presence of bacteria within the stones was detected with electron microscopy.<sup>10</sup> The most detected bacterial species belong to the *Streptococcus* genus, whose species are part of the oral microbiome.<sup>11</sup> Similarly, bacteria are also found in many brown pigment stones and cholesterol gallstones,<sup>12,13</sup> as well as in kidney stones,<sup>14</sup> and it is believed that the formation of these stones is often due to biofilm, even in the absence of evident inflammatory processes.

Assuming that a retrograde migration of food, bacteria, and foreign bodies from the oral cavity to salivary ducts does occur, the aim of this study was to evaluate the presence of bacteria and/or biofilm in salivary gland stones, even in the absence of clinically apparent sialadenitis. We believe that bacteria and biofilm organic matrix play a key role in calculus formation. To this purpose, salivary gland stones, collected from patient samples negative for acute sialadenitis, were analyzed for the presence of biofilm and bacteria.

## Materials and Methods

### Patients

In the present study, 15 salivary gland stones were selected from 12 patients: all had at least 1 salivary colic episode; 2 of these (3 salivary gland stones) presented with repeated episodes of salivary colic during the 6-month period before diagnosis. Calculi ranged from 2 to 8 mm in size. The samples were collected at the Sapienza University of Rome, Department of Sensory Organs, ENT Clinic, and the Department of Surgical Biotechnologies and Science, ENT Section, and sectioned into 2 parts in a sterile environment. The samples were analyzed for the presence of bacterial biofilm matrix and bacteria via traditional optic microscopy and scanning electron microscopy (SEM). Furthermore, at the Department of Public Health and Infectious Diseases, Microbiology Section, quantitative real-time PCR (qPCR) assays were carried out. This case series study was approved by the institutional review board of the Policlinico Umberto I Hospital of Rome prior to conducting the study.

### Microscopy

The stones underwent decalcification via EDTA disodium in an acid buffer (Osteodec Bio-Optica, Milano, Italy) for 48 hours. Later, the stones were sectioned into 2 parts and prepared as follows.

**Optic microscopy.** One half of each stone was first rinsed in distilled water, processed, and embedded in paraffin. For each salivary gland stone, 2- $\mu$ m-thick serial sections were obtained with a rotary microtome (Leica, Wetzlar, Germany). The sections were then mounted onto positively charged glass slides (SuperFrost, London, UK). Each specimen was stained with

hematoxylin and eosin as well as special staining, such as Gram, Giemsa, PAS (periodic acid–Schiff), and alcian-PAS.

**Scanning electron microscopy.** The other halves of the stones were fixed on an aluminum stub by a silver conductive paste (Silver Paint; TAAB, Berkshire, UK), which helps the stone adhere to the stub and conduct incident electrons during SEM observation. The samples were then placed in the K550 Sputter Coater and metalized at a 10-mA current for 3 minutes. The stones were then ready for SEM evaluation (Hitachi S-4000) with digital image acquisition software for every SEM image (DISS 5).

**DNA extraction from salivary gland stone sections.** Total DNA was extracted from 5- to 6- $\mu$ m sections obtained from the paraffin-fixed stone halves. Total DNA was extracted with the dedicated DNeasy Tissue Kit (Qiagen, Hilden, Germany) following the manufacturer's instructions for DNA extraction from formalin-fixed, paraffin-embedded (FFPE) tissues. Starting material included ten 4- $\mu$ m-thick microtomed slices (approximately 50-80 mg of tissue). To obtain maximum yield of both Gram-positive and Gram-negative bacteria, a special step in DNA purification protocol was added. Briefly, 180  $\mu$ L of ATL buffer was added to samples, followed by 180- $\mu$ L volume of enzymatic lysis buffer (20mM TrisHCl, pH 8.0, 2mM sodium EDTA, 1.2% Triton X-100, lysozyme to 20 mg/mL), and incubated for 30 minutes at 37°C; 25  $\mu$ L of proteinase K solution and 200  $\mu$ L of buffer AL were then added, followed by a 30-minute incubation step at 56°C. DNA concentration was determined with Eppendorf Biophotometer at 260 nm and integrity checked through 1% agarose gel electrophoresis containing EtBr, 0.5  $\mu$ g/mL.

**qPCR assays and conditions.** qPCR was employed. Primers were commercially synthesized by Biofab Research (Rome, Italy) based on the following sequences: total bacteria, F 5'-ACTCCTACGGGAGGCAGCAGT-3'; total bacteria, R 5'-ATTACCGCGGCTGCTGGC-3'. qPCR amplifications were carried out in a volume of 25  $\mu$ L with 10mM Tris-HCl (pH 8.8), 2mM MgCl<sub>2</sub>, 100 $\mu$ M each dNTP, 0.5 $\mu$ M each primer, 0.6 U of SensiMix SYBR Hi-ROX Kit (Bioline, London, UK), and 5  $\mu$ L of template (corresponding to approximately 200 ng of DNA). Negative and positive controls were also employed. A standard curve was generated by means of 10-fold serial dilutions of a starting amount of PCR-amplified DNA (200 ng). Running conditions were 95°C for 10 minutes, 40 cycles at 95°C for 20 seconds, 60°C for 20 seconds, 72°C for 27 seconds, and a final dissociation stage implemented automatically by the thermocycler 7300 Real-Time PCR System (Applied Biosystems, Foster City, California).

## Results

### Optical Microscope Observation

Optical microscope observation of histologic sections showed formations that, due to their size, shape, and Gram and Giemsa staining, seemed to be Gram-positive

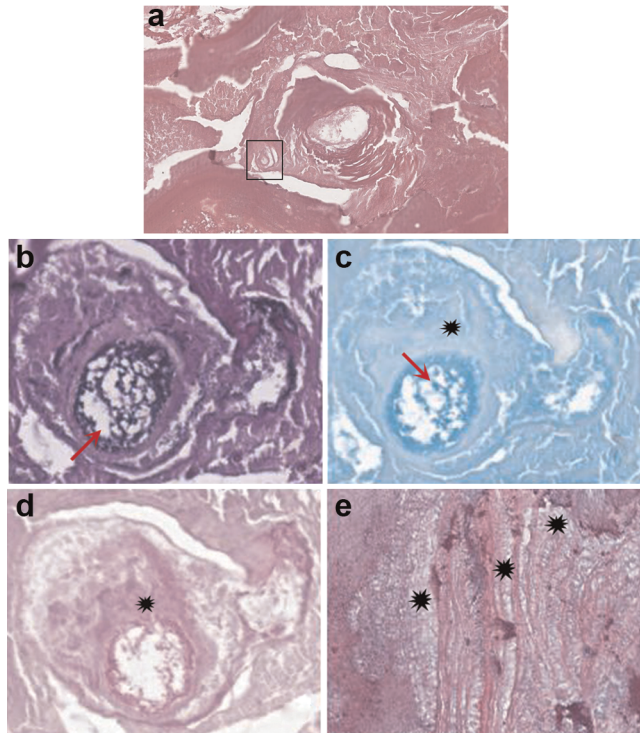


**Figure 1.** (a) Hematoxylin and eosin. Small stone with a central multilacunar area where bacteria have been found surrounded by amorphous material (10× magnification). (b, c) Low-power (40×) magnification. Positivity for special stains Gram and PAS (periodic acid–Schiff). Small stone with central multilacunar areas where an amorphous material (\*) deposit resembling bacteria in shape is present (arrow). (d) Low-power (40×) magnification. (e) High-power (70×) magnification. Staining by Giemsa and alcian-PAS of the amorphous material (\*). The tissue appears to be organized in lamellar layers.

bacterial cells (**Figure 1b, 1c**). PAS staining, in which the most apparent components are those of the carbohydrate glycocalyx, and PAS-positive staining matrix around the bacteria were observed, this matrix being even more evident after alcian-PAS staining (**Figure 1d, 1e**), which defines the core and outer layers of the stone. We observed an amorphous stain substance around the supposed Gram-positive bacterial forms. On the edges of the stone, precipitates of calcareous concretions were deposited in layers with a lamellar-like pattern (Fig. 1d, 1e). This is consistent with the optical microscope appearance of biofilm.

### SEM Observation

The ultrastructural observation of the material processed for SEM showed the presence of forms that resembled bacterial cells in the middle of the stones, surrounded by soft amorphous material with a lamellar-like aspect, mixed with deposits of inorganic precipitates (**Figure 2** insert). The bacterial forms appeared as isolated bacterial cells and bacteria aggregates in colonies, improving the results obtained by Gram-staining optic microscopy.

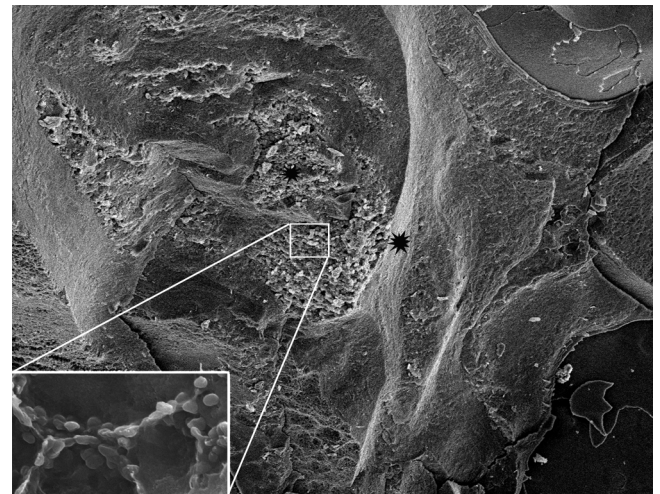


**Figure 2.** Scanning electron microscopy, 1000× magnification. Core of the stone where bacterial-like bodies surrounded by amorphous material are detected (\*). Insert: 6000×, high power.

### qPCR assay

Bacterial universal primers were used to amplify a 172–base pair region of the bacterial 16S rDNA, and the total DNA extracted from the FFPE tissue sample (approximately 50–80 mg) was used as a template. qPCR results showed the presence of approximately 1.03 pg of amplified bacterial DNA in the FFPE tissue sample. Taking into consideration that a single prototype bacterial genome weighs on average 3.254 fg and that the average number of 16S rDNA operons is 7, 1.03 pg of amplified DNA corresponded to approximately  $7 \times 10^5$  bacterial cells per approximately 50 to 80 mg of tissue. Although our results are not comparable with a recent study highlighting that in 600  $\mu$ L of saliva there were approximately 70,000 bacteria, it can be argued that there is a 10:1 bacterial density ratio in calculi.<sup>15</sup>

### Discussion

In previous electron microscopy<sup>10</sup> and DNA PCR studies, analysis of salivary glands<sup>11</sup> demonstrated that bacteria were occasionally present in salivary gland stones. Some authors also demonstrated the presence of an organic matrix in the stones, composed of carbohydrates and amino acids, interpreted as mucous plug precipitation in the oversaturation solution.<sup>2,9–11</sup>

The aim of the present study was to evaluate the presence of bacteria and/or bacterial biofilm in stones of salivary gland ducts. Traditional optic microscopy from gland stone samples revealed images resembling Gram-positive bacterial cells. SEM observations showed the same results. qPCR performed on the middle slices of stones confirmed the presence of bacterial DNA.

Both optic and SEM microscopy showed that the bacterial-like forms and the organic material surrounding them were situated in the middle of the stone, indicating the presence of aggregation nuclei of inorganic material (**Figure 1d**). These nuclei were sometimes enclosed in

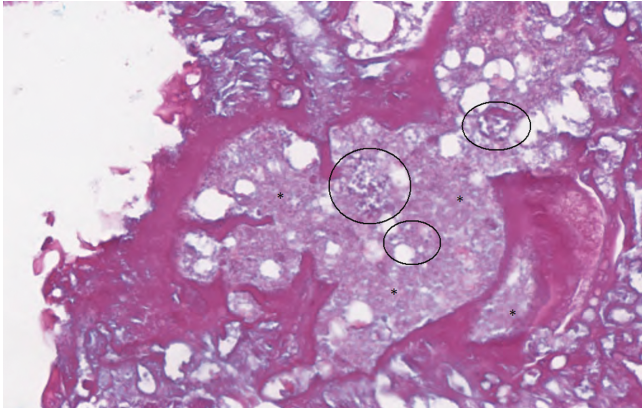


**Figure 3.** Alcian-PAS (periodic acid–Schiff). High-power (40×) magnification. Organic material is highlighted by alcian-PAS staining, indicating the glycoprotein nature of the matrix (\*). Within the circles, bacterial-like bodies are observed.

outer concentric inorganic layers (**Figure 1e**). Brady et al also showed the presence of bacteria in the core of the salivary stones.<sup>10</sup> Finally, alcian-PAS positivity observed in the organic material (**Figure 3**) highlights the glycoprotein nature of the matrix, in which the presence of bacterial-like cells is also possible. The organic substance surrounds bacteria and is in turn surrounded by inorganic substance without mixing, which is what characterizes the classic theory.

In conclusion, our results suggest that the presence of bacteria in the salivary stones, surrounded by organic matrix having a glycoprotein component, indicates a biofilm organization. The biofilm organization is supported by SEM images presenting a geometric distribution of bacteria within the organic matrix, which is typical of the same kind of biofilm structure.<sup>16</sup> The biofilm polysaccharide matrix is negatively charged and is capable of attracting bivalent cations available in aqueous solutions, such as saliva. The bivalent recruited cations, such as calcium, magnesium, and iron, are subsequently used for the formation of a chemical bridge among the polymeric chains that will form the matrix that protects the microorganisms.<sup>17,18</sup> Carbonates and phosphates may be present among the exchanged anions, forming crystal nuclei of the corresponding calcium salts, which will trigger mineralization/concretion from which lithiasis originates.<sup>19-21</sup>

Considering the topography of colonization, principally in the middle area of the stones, it may be hypothesized, as already reported by Marchal et al, that bacteria and microbe biofilm may play a role in lithiasic formation, contrary to when it is recovered from the outer layers of the stones, where it may be a consequence of the lithiasic formation.<sup>3</sup>

Our thesis highlights the similarity of calculus formation among salivary glands, gallbladder, and kidneys. The formation of gallstones may be caused by an infectious process that can evolve in both types of stones: cholesterol gallstones or brown pigment stones. Although the exact contribution of bacteria to lithogenesis is not completely understood, the clinician should be aware that most gallstones are colonized by a

bacterial biofilm, even when bile cultures are negative.<sup>13</sup> Biofilm also plays an important role in kidney stone pathogenesis. Unexpectedly, urinary sepsis was not a constant finding in these patients during clinical follow-up.<sup>14</sup> Positive urine cultures were found in only 20% of struvite formation cases; however, in these cases, biofilm was found in as much as 50% of the calculi formations. This “anomalous” culture negativity may be explained by a low microbe load or by the absence of planktonic bacteria colonizing struvite formation in a “biofilm lifestyle.”<sup>22,23</sup>

Further studies are necessary to improve our results and to better understand the bacterial role in the lithiasic process, yet our findings strongly suggest the presence of microbes organized in a biofilm pattern, especially in the middle of salivary stones where it may be the consequence of an infective process or a simple bacteria colonization of the salivary duct. Both may act as nuclei-organizing and lithiasis-inducing events.

## Conclusions

To explain the etiopathogenesis of sialolithiasis, the most commonly accepted hypotheses are “the classic theory” (ie, the calcium microconcretions with an intracellular origin) and “the retrograde theory.” We have shown the presence of bacterial DNA and a structure resembling bacterial biofilm in salivary gland stones, which, depending on the biofilm’s location, may be considered the cause and/or consequence of lithiasis in both cases. Our findings mainly refer to the middle of the stone, stressing the causative role of the bacteria (eg, crystallization nuclei) in the lithiasis process. Further research is necessary to confirm our results and to answer the question, is bacterial biofilm in salivary gland stones the cause or the consequence?

However, this study opens a new horizon for future investigations, aimed to confirm the retrograde theory and to better clarify the role of bacteria in the formation and/or pathogenesis of salivary gland stones.

## Author Contributions

**Massimo Fusconi**, editorial manager, data analysis, drafting, final approval, accountability for all aspects of the work; **Vincenzo Petrozza**, data analysis, drafting, final approval, accountability for all aspects of the work; **Serena Schippa**, data analysis, drafting, final approval, accountability for all aspects of the work; **Marco de Vincentiis**, data analysis, drafting, final approval, accountability for all aspects of the work; **Giuseppe Familiari**, data analysis, drafting, final approval, accountability for all aspects of the work; **Fabrizio Pantanella**, data analysis, drafting, final approval, accountability for all aspects of the work; **Mirko Cirenza**, data analysis, drafting, final approval, accountability for all aspects of the work; **Valerio Iebba**, data analysis, drafting, final approval, accountability for all aspects of the work; **Ezio Battaglione**, data analysis, drafting, final approval, accountability for all aspects of the work; **Antonio Greco**, data analysis, drafting, final approval, accountability for all aspects of the work; **Camilla Gallipoli**, data analysis, drafting, final approval, accountability for all aspects of the work; **Flaminia Campo**, data analysis, drafting, final approval, accountability for all aspects of the work; **Andrea Gallo**, data

analysis, drafting, final approval, accountability for all aspects of the work.

## Disclosures

**Competing interests:** None.

**Sponsorships:** None.

**Funding source:** None.

## References

1. Epivatianos A, Harrison JD, Dimitriou T. Ultrastructural and histochemical observations on microcalculi in chronic submandibular sialadenitis. *J Oral Pathol*. 1987;16:514-517.
2. Harrison JD, Triantafyllou A, Baldwin D, Schäfer H. Histochemical and biochemical determination of calcium in salivary glands with particular reference to chronic submandibular sialadenitis. *Virchows Arch A Pathol Anat Histopathol*. 1993;423:29-32.
3. Marchal F, Kurt AM, Dulguerov P, Lehmann W. Retrograde theory in sialolithiasis formation. *Arch Otolaryngol Head Neck Surg*. 2001;127:66-68.
4. Takeshita H, Ishihara A, Yamashita T, Itoh A, Yoshida K, Fukaya M. A case of salivary calculus containing a limb of a shrimp: the structural analysis. *Aichi Gakuin Dent Sci*. 1990;3:49-58.
5. Pratt LW. Foreign body in Wharton's duct with calculus formation. *Ann Otol Rhinol Laryngol*. 1968;77:88-93.
6. Watkins RM. Submandibular salivary duct calculus secondary to a foreign body. *Br J Surg*. 1982;69:379.
7. Yamamoto H, Sakae T, Takagi M, Otake S. Scanning electron microscopic and X-ray microdiffractometric studies on sialolith-crystals in human submandibular glands. *Acta Pathol Jpn*. 1984;34:47-53.
8. Ashby RA. The chemistry of sialoliths: stones and their homes. In: Norman JED, McGurk M, eds. *Color Atlas and Text of the Salivary Glands: Diseases, Disorders, and Surgery*. London, UK: Mosby-Wolfe; 1995:243-251.
9. Teymoortash A, Wollstein AC, Lippert BM, Peldszus R, Werner JA. Bacteria and pathogenesis of human salivary calculus. *Acta Otolaryngol*. 2002;122:210-214.
10. Brady JM, McKinney L, Stanback JS. Scanning electron microscopy of submandibular sialoliths: a preliminary report. *Dentomaxillofac Radiol*. 1989;18:42-44.
11. Teymoortash A, Wollstein AC, Lippert BM, Peldszus R, Werner JA. Bacteria and pathogenesis of human salivary calculus. *Acta Otolaryngol*. 2002;122:210-214.
12. Parsek MR, Singh PK. Bacterial biofilms: an emerging link to disease pathogenesis. *Annu Rev Microbiol*. 2003;57:677-701.
13. Swidsinski A, Lee SP. The role of bacteria in gallstone pathogenesis. *Front Biosci*. 2001;6:E93-E103.
14. Grigoryan L, Trautner BW, Gupta K. Diagnosis and management of urinary tract infections in the outpatient setting: a review. *JAMA*. 2014;312:1677-1684.
15. Dassi E, Ballarini A, Covello G, et al. Enhanced microbial diversity in the saliva microbiome induced by short-term probiotic intake revealed by 16S rRNA sequencing on the IonTorrent PGM platform. *J Biotechnol*. 2014;190:30-39.
16. Triantafyllou A. *Microolithiasis of the Major Salivary Glands of Cat: A Morphological, Histochemical and Biochemical Study* [PhD thesis]. London, UK: University of London; 1991.
17. Triantafyllou A, Harrison JD, Garrett JR, Kidd A. Increase of microliths in inactive salivary glands of cat. *Arch Oral Biol*. 1992;37:663-666.
18. Flannigan R, Choy WH, Chew B, Lange D. Renal struvite stones: pathogenesis, microbiology, and management strategies. *Nat Rev Urol*. 2014;11:333-341.
19. Bower CK, McGuire J, Daeschel MA. The adhesion and detachment of bacteria and spores on food-contact surfaces. *Trends Food Sci Technol*. 1996;7:152-157.
20. Characklis WJ, Marshall KC. *Biofilms*. Hoboken, NJ: John Wiley & Sons; 1990.
21. Saez R, Rittmann J. Improved pseudoanalytical solution for steady-state biofilm kinetics. *Biotechnol Bioeng*. 1987;32:379-385.
22. Zanetti G, Paparella S, Trinchieri A, Prezioso D, Rocco F, Naber KG. Infections and urolithiasis: current clinical evidence in prophylaxis and antibiotic therapy. *Arch Ital Urol Androl*. 2008;80:5-12.
23. Klaus-Joerger T, Joerger R, Olsson E, Granqvist CG. Bacteria as workers in the living factory: metal-accumulating bacteria and their potential for materials. *Trends Biotechnol*. 2001;19:15-20.